



Contents lists available at [ScienceDirect](#)

Chemical Physics Letters

journal homepage: www.elsevier.com/locate/cplett



Erratum

Erratum to: 'Molecular dynamics simulations of an apolipoprotein A-I derived peptide in explicit water' [Chem. Phys. Lett. 461 (2008) 294]

Athanassios Stavrakoudis*

Department of Economics, University of Ioannina, Panepistimioupoli, 45110 Ioannina, Greece

The word 'apolipoprotein' in the title and abstract (lines 1 and 6) of the article has to be replaced by 'apolipoprotein'. Therefore,

the title of the article is 'Molecular dynamics simulations of an apolipoprotein A-I derived peptide in explicit water'.

DOI of original article: [10.1016/j.cplett.2008.07.007](https://doi.org/10.1016/j.cplett.2008.07.007)

* Fax: +30 265 109 5092.

E-mail address: astavrak@cc.uoi.gr

URL: <http://stavrakoudis.econ.uoi.gr/>



Molecular dynamics simulations of an apolipoprotein A-I derived peptide in explicit water

Athanassios Stavrakoudis *

Department of Economics, University of Ioannina, 45110 Ioannina, Greece

ARTICLE INFO

Article history:

Received 31 March 2008

In final form 1 July 2008

Available online 8 July 2008

ABSTRACT

Molecular dynamics simulations have been performed for the 104–117 α -helical fragment of apolipoprotein A-I using the CHARMM22 force field and the NAMD simulation engine. Simulation (50 ns in explicit water) resulted in significant appearance of π -helix conformation, which was totally diminished when the CMAP correction of the CHARMM force field was applied. This is consistent with other similar studies which suggest that the observation of π -helix in peptide conformation was force field biased rather actually existed. This study suggests that the 104–117 fragment of apolipoprotein A-I has a stable α -helical conformation in water.

© 2008 Elsevier B.V. All rights reserved.

1. Introduction

About one third of amino acid residues in proteins are found in helical conformation. There are three main type helices found in crystal structure of proteins, which are classified as (a) α -helix or 3_6 -helix, (b) 3_{10} -helix and (c) π -helix or 4_4 -helix. The α -helix, originally proposed by Pauling and Corey, is the most abundant, while π -helix is only rarely found. Occurrence of π -helix has been questioned. This secondary structure has a large entropic cost of formation [1], since the $i \leftarrow i + 5$ hydrogen bond pattern needs five consecutive residues to be properly rearranged.

There are numerous studies during last years that reconsider the occurrence frequency and importance of π -helical conformation [2]. Despite the geometrically and energetically unfavorable factors that previously mentioned, experimental and theoretical studies reveal π -helical conformations in solution to be existed. Interestingly, a recent investigation based on structure analysis of PDB deposited crystal structures reveals that π -helix is significantly more prevalent than previously thought [2]. Molecular dynamics simulations of alamethicin [3], (AAXAA)₃ peptides, mutant c-erbB2 peptide [4], Fe(III) mesoporphyrin derived peptide [5], central domain of smooth muscle caldesmon [6] and transmembrane region of tyrosine kinase receptor (NeuTM35) [7], revealed π -helical conformations to be in presence. The last case was experimentally confirmed by NMR [8]. There is also a noticeable case were a Zn²⁺-binding peptide adopts a π -helix conformation in solution, as suggested by NMR [9].

ApoA-I is a member of lipoproteins family and plays an important role in reverse cholesterol transport [10,11]. Helical fragments from apoA-I sequence has attracted considerable interest [12,13] from researchers in order to elucidate their particular functional properties. This study presents simulation based results of the solution conformation of a helical fragment derived from the helix-4 of apoA-I [14]. The capped peptide Ac-F¹⁰⁴QKKWQEEM-ELYRQ¹¹⁷-NH₂ that corresponds to the 104–117 sequence of apoA-I is studied with molecular dynamics simulation in explicit water for 50 ns. The CHARMM22 [15] and CHARMM22/CMAP [16] force fields were applied. Under the light of the current study the peptide retained its helical structure in aqueous solution. As in other reported cases, α - to π -helix transitions recorded with the CHARMM22 force field. Anyway this is most possibly an artifact caused by the force field parameterization since the application of the CHARMM22/CMAP force field eliminated the π -helix occurrence.

2. Computational methods

Initial coordinates of the apoA-I crystal structure were downloaded from the Protein Data Bank [17], PDB access code: 1AV1. Two identical simulations were set up (with subsequent names S1 and S2) differing only on the force field parameters. All MM/MD calculations were performed with NAMD 2.6 [18] package. Topology and force field parameters were assigned from the CHARMM22 protein parameter set [15] for the S1 simulation and from CHARMM22/CMAP [16] for the S2 simulation. The fragment 104–117 was extracted from chain A and hydrogen atoms were added with the VMD program [19]. Acetyl and amide patches were employed at N- and C- terminus of the peptide, respectively. The peptide was solvated in a box with dimensions

* Fax: +30 265 109 5092.

E-mail address: astavrak@cc.uoi.gr

URL: <http://stavrakoudis.econ.uoi.gr/>

$5.27 \times 5.66 \times 5.75 \text{ nm}^3$, containing TIP3P [20] water molecules. The size of the box allowed a minimum distance of 1.8 nm between any protein atom and the edge of the box. The big sized solvent box has been shown to be essential in order to avoid the periodicity-induced artifacts, when the PME method is applied for electrostatic calculations [21]. Twelve pairs of Na^+ and Cl^- ions were added to the system, using VMD's autoionize plugin. The final simulated box contained 5257 water molecules. Periodic boundary conditions were employed to the system. Van der Waals interactions were gradually turned off at a distance between 1.0 and 1.2 nm. The non-bonded pair list was updated every 10 steps. Long range electrostatics were computed every two steps with the PME method [22,23], with a grid spacing of less than 0.1 nm and fourth order b-spline interpolation was used to calculate the potential and forces in between grid points. Bonds to hydrogen atoms were constrained by applying the SHAKE [24,25] method with a relative tolerance of 10^{-8} , allowing a 2 fs step for integration time step. The whole system, consisted by 16069 atoms, was energy minimized with 2500 steps of conjugate gradients, by keeping the coordinates of protein heavy atoms fixed at the crystallographic positions. After minimization, the temperature of the system was gradually increased with Langevin dynamics [26], using the NVT ensemble, to 310 K, during a period 3000 steps, by stepwise reassignment of velocities every 500 steps. Equilibration at 310 K was continued until 200 ps. During this period the positions of the protein heavy atoms were restrained to crystallographic original coordinates with a force of $50 \text{ kcal mol}^{-1} \text{ \AA}^{-2}$. Equilibration at 310 K was continued for another 300 ps without any restraints applied to the system. The simulation was continued to the production phase, under constant pressure, with Langevin piston method [27], thus NPT ensemble, for 50 ns. Pressure was maintained at 1 atm and temperature was kept at 310 K. The results presented here are from this, isothermal–isobaric ensemble, MD run. Snapshots were saved to disk at 1 ps interval for further analysis. Conformation analysis and visual inspection of structures were performed with VMD [19], and CARMA [28] software packages, along with some in-house Octave code. Secondary structure assignment was performed with STRIDE [29]. Structural figures were prepared with PYMOL [30].

The peptide's conformational stability was also checked with AMBER99 force field [31]. Simulation (S3) was performed with the TINKER software package [32]. The SASA implicit solvation model was used [33]. Cutoff values were set to 0.15 nm for electrostatic interactions and 0.12 nm for van der Waals interactions. The starting conformation (same as described previously) was minimized for 100 steps and subsequently subjected to molecular dynamics (at 310 K) for 80 ns. 8000 structures were saved for analysis in this case.

3. Results and discussion

3.1. Analysis of the crystal structure

The crystal structure of the 104–117 fragment of apoA-I is found in α -helix conformation with regular $i \leftarrow i + 4$ hydrogen bond network. The backbone dihedral angles are given in Table 1. The helix is further stabilized by side chain interactions of both electrostatic and hydrophobic nature. The distances between side chain charge centers were found 0.77 nm for Lys106: N_ϵ –Glu110: C_δ , 0.71 nm for Lys107: N_ϵ –Glu111: C_δ and 1.29 nm for Lys106: N_ϵ –Glu111: C_δ . There are also some key hydrophobic interactions, for example distances of Phe104: $\text{C}_{\epsilon 1}$ –Trp108: $\text{C}_{\zeta 2}$, Trp108: $\text{C}_{\zeta 2}$ –Met112: C_β , Met112: S_δ –Tyr115: C_β are 0.45, 0.40 and 0.53 nm, respectively. Superimposition of the resulted structures (last frame) on the crystal structure is shown in Fig. 1.

Table 1

Backbone dihedral angles as computed from PDB structure and averaged over S1 and S2 molecular dynamics trajectories

Residue	Backbone dihedral angle					
	PDB		S1		S2	
	ϕ	ψ	ϕ	ψ	ϕ	ψ
Gln105	−52.4	−47.7	−67.7	−46.8	−82.4	63.3
Lys106	−64.6	−27.4	−67.9	−48.9	−62.6	−42.3
Lys107	−64.5	−41.8	−73.7	−52.6	−67.4	−36.3
Trp108	−67.0	−43.9	−75.6	−51.6	−64.0	−42.0
Gln109	−53.2	−31.6	−73.5	−51.1	−64.6	−40.0
Glu110	−68.3	−55.3	−74.9	−60.6	−63.3	−42.2
Glu111	−62.4	−44.5	−66.3	−54.5	−64.7	−40.7
Met112	−43.4	−65.0	−70.0	−59.6	−63.4	−41.0
Glu113	−50.5	−45.3	−70.6	−50.6	−63.6	−40.9
Leu114	−52.8	−46.0	−77.1	−57.7	−64.9	−38.8
Tyr115	−69.0	−47.2	−80.1	−55.5	−66.8	−36.7
Arg116	−52.6	26.0	−73.5	−57.8	−85.6	−6.0

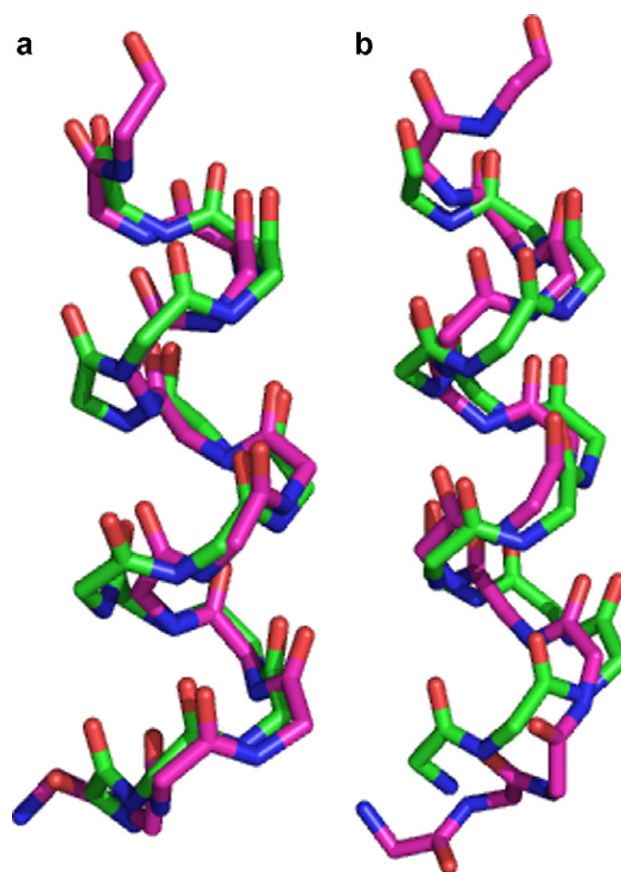


Fig. 1. Backbone superimposition of frames from S1 (pink) and S2 (green) simulations at (a) 10 ns and (b) 45 ns, demonstrating the partial and almost total π -helical conformation observed during S1. (For interpretation of the references to colour in this figure legend, the reader is referred to the web version of this article.)

3.2. RMSD and C_α distances

The backbone RMSD time evolution for peptide's backbone atoms over the 50 ns trajectory from the starting conformation (crystal structure) is shown in Fig. 2. It is clearly seen that for the CHARMM22 case (S1 simulation) a structural change occurred at approximately 7.5 ns. After this jump of RMSD from approximately 0.16 nm to 0.3 nm, over a period of less than 1 ns, this value remained constant close to 0.3 nm. RMSD values from the S2

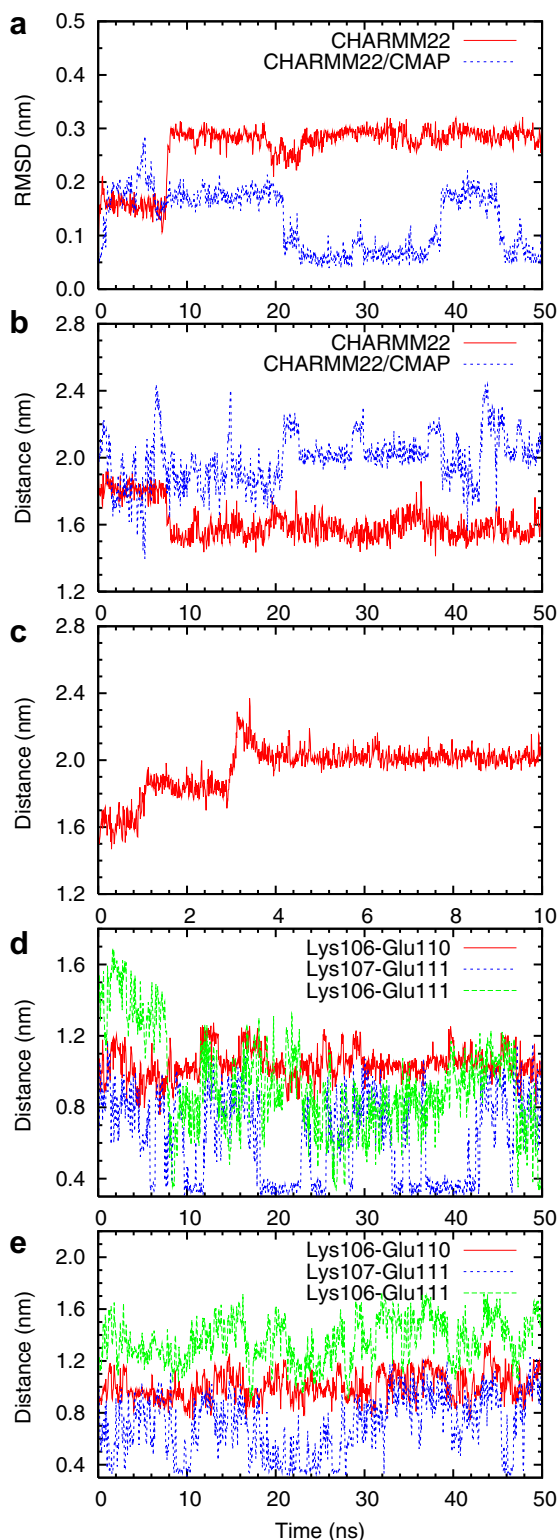


Fig. 2. Trajectory time evolution of (a) RMSD of backbone atoms, (b) distance of Phe104:C α -Gln117:C α atoms, (c) distance of Phe104:C α -Gln117:C α atoms after the extension of S1 trajectory with CHARMM22/CMAP, (d) side chain distances in S1 (CHARMM22) experiment and (e) side chain distances in S2 (CHARMM22/CMAP) simulation. C δ and N ϵ atoms of Glu and Lys residues, respectively, were used as side chain charge centers.

simulation were found around 1.8 nm for approximately half of the trajectory, or 0.6 nm for the other half. Thus conformational changes during S2 simulation were smoother than S1 and lower

Table 2

Percentage of occurrence of secondary structure states of individual residues during S1 and S3 simulations

Residue	% of conformational state			
	Coil	π -Helix	Turn	α -Helix
Phe104	0.1	33.2	17.4	49.3
Gln105	0.1	32.2	17.0	48.7
Lys106	0.1	39.3	11.3	49.3
Lys107	0.0	41.4	8.5	50.2
Trp108	0.0	41.8	6.8	51.4
Gln109	1.5	33.0	5.8	59.8
Glu110	2.1	48.0	2.9	47.1
Glu111	2.1	53.9	1.8	42.2
Met112	2.1	56.0	1.4	40.4
Glu113	2.2	55.6	3.0	39.3
Leu114	26.9	31.2	4.2	37.7
Tyr115	53.6	16.2	4.1	26.2
Arg116	85.6	4.2	3.6	6.7
Gln117	100.0	0.0	0.0	0.0

RMSD values indicate that the peptide's backbone structure remained closer to the initial α -helical conformation.

This structural change during S1 simulation is also confirmed by the end-to-end distance, measured between the C α atoms of residues Phe104 and Gln117. The change in distance, between C α of Phe104 and C α of Gln117 atoms, is seen at approximately 7.5 ns. During the first 7 ns of simulation, this distance fluctuates with a mean value of 1.81 nm, while after 8 ns of simulation and until the end (50 ns), this value is shifted downwards to mean value of 1.58 nm. This value is considerable lower than the distance that corresponds to an ideal α -helix of a 14mer peptide, which is 2.1 nm, if 0.15 nm is taken as the step distance per residue. Indeed, it is even shorter from 1.68 nm, which is the corresponding distance for a 14-residue ideal π -helix.

This structural change is not uniformly distributed throughout the peptide sequence. The C-terminal is more susceptible to conformational changes, while the N-terminal fragment remains more solid. The six-residue N-terminal part of the peptide remained in the α -helix conformation in rather bigger time, than the 8-residue C-terminal part (Table 2). The backbone RMSD of the N-terminal fragment fluctuated around 0.12 nm throughout the whole simulation period, while the value of the corresponding C-terminal fragment backbone RMSD, shifted from 0.05 nm during the first 7 ns of simulation to approximately 0.2 nm after the 9th ns of simulation. These facts let us hypothesize that the structural change of the peptide around 7.5 ns can be ascribed to the C-terminal fragment.

On the other hand, the corresponding end-to-end distance during the S2 simulation fluctuated with mean value of 1.9 nm (very close to the ideal value of 2.1 nm) and standard deviation of 1.5 nm. Some short-timed jumps to extreme values like 2.4 or 1.5 nm have been also recorded but the peptide's end-to-end distance quickly returned to the equilibrium values.

3.3. Backbone dihedral angle analysis

Backbone dihedral angles of starting conformation, as well as trajectory averages are presented in Table 1. During the first 7 ns of the S1 simulation, average backbone dihedral angles of the fragment Gln105–Glu111 remain remarkably close to the corresponding values of the starting conformation. On the contrary, residues Glu113–Arg116 have average φ and ψ values considerably shifted from the starting values. For example (φ , ψ) values of Leu114 are (-53° , -46°) in the crystal structure, while they average at (-81° , -54°) during the first 7 ns.

Simulation S2 on the other side totally eliminated the backbone dihedral transitions outside of the α -helix region. As it can be seen

from Table 1, most (φ , ψ) angles fluctuated around (-65° , -40°) values. The most notable exception was from the ψ_{105} . This dihedral angle showed preference for values either around -40° for half of the trajectory or around -140° for the other half. The corresponding value from crystal structure was -48° . During simulation time four main transitions occurred: (a) from $\sim -40^\circ$ to $\sim -160^\circ$ during first ns of simulation, (b) from -160° to -40° during 21st ns, (c) from -40° to $\sim -160^\circ$ at 38th ns and (d) from $\sim -40^\circ$ to $\sim -160^\circ$ at 46th ns. The profile of these transitions fits well when the corresponding profile of the RMSD (Fig. 2).

3.4. Secondary structure analysis

Table 3 lists the secondary structure assignment for individual residues, during S1 simulation. These structural assignments were also clustered for the whole sequence and the results are presented in Table 3. It is interesting to note that most of the residues spend most of the time in α -helical conformation during S1 MD trajectory. This is more evident for the residues close to N-terminal end. The two C-terminal residues adopt mainly the coil conformation which is consistent with previous studies [34] and can be attributed to the greater flexibility of helix termini due to less possible backbone hydrogen bonds. This indicates that π -helix is not more stable conformation for the peptide under the simulation conditions, but rather that there is a balance between α - and π -helix. Time series analysis of the secondary structure revealed that after the 8th ns, the peptide undergoes numerous transitions between α - and π -helix. Most of residues are also found in turn conformation between transition events, as have been reported in other cases [6]. It is noticeable that turn state is more frequently found between helix transitions in residues close to N- or C-terminus.

The residues of the N-terminal part of the peptide (fragment Phe104–Glu109) adopt cooperative transitions during the trajectory in an almost perfect manner. After the first transition at approximately 7.5 ps they remain (most of the time) in π -helix conformation for about 11 ns and they return back to α -helical conformation. The later transition is not observed for residues Met112–Gln117, while residues Gln109–Glu110 adopt partly the α -helical conformation during the period 18th to 23rd ns. After the 23rd ns, the transitions between α - and π -helical conformations are very frequent.

Table 4 lists the number of transitions found in the S2 trajectory and the percentage of occurrence of the main transitional paths. As

Table 4
Conformational transitions of individual residues observed during S1 simulation

Residue	Total Number	Conformational transitions			
		H \rightarrow I	H \rightarrow T \rightarrow I	I \rightarrow H	I \rightarrow T \rightarrow H
Gln105	15471	14.5	4.2	14.3	4.4
Lys106	14908	23.0	3.5	22.7	3.8
Lys107	14151	27.0	3.2	27.0	3.3
Trp108	13893	30.7	2.9	30.5	3.1
Gln109	17404	32.5	2.5	32.2	2.7
Glu110	17136	37.2	1.3	36.9	1.4
Glu111	17211	39.9	0.8	39.7	0.8
Met112	16766	40.7	0.5	40.5	0.6
Glu113	17378	37.2	1.1	37.0	1.2
Leu114	22087	16.6	0.6	16.5	0.7
Tyr115	19990	6.9	0.3	6.8	0.3
Arg116	10398	1.3	0.1	1.1	0.1

First column lists the peptide's residue, second column lists the total number of conformational transitions and the rest of columns list the percentage of specific conformational transition paths.

it has been observed previously [6], α - to π -helical transitions involve passage through turn conformation. A closer look at Table 4 reveals that transitions from α - to π - or from π - to α - transitions can occur without turn intermediates. In fact, for most of the residues (mainly those on the central part of the peptide) direct transitions between the two helical types was observed. Coil and turn conformational states between helical transitions were also observed but to a lower extent.

Results from S2 trajectory revealed that the peptide remained in α -helical conformation for 100% of the time. Only the C-terminal Gln117 was found in coil conformation, something that is very frequent in similar cases. The helix stability is in agreement with previously analyzed results for backbone dihedrals.

3.5. Backbone hydrogen bonds

Since helices are stabilized through backbone hydrogen bond network, it is very interesting to look at the peptide's backbone hydrogen bonds. Table 5 lists the percentage of hydrogen bonds found during S1 trajectory that correspond to 3_{10} -, α - or π -helix. In line with other reported results in the literature, hydrogen bond network in S1 simulation seems to favor π -helical conformation. The $i \leftarrow i+5$ hydrogen bond pattern become dominant as the peptide had approximately 5–8 such hydrogen bonds. On the

Table 3
Secondary structure clusters during S1 (CHARMM22) and S3 simulations (AMBER99)

	Sequence and secondary structure ^a														% Occurrence
	W	Q	K	K	W	Q	E	E	M	E	L	Y	R	Q	
Cluster S1															
1	I	I	I	I	I	I	I	I	I	I	C	C	C	C	22.3
2	H	H	H	H	H	H	H	H	H	H	H	H	C	C	14.1
3	H	H	H	H	H	H	I	I	I	I	I	C	C	C	13.0
4	T	T	I	I	I	I	I	I	I	I	I	I	C	C	5.4
5	H	H	H	H	H	H	H	H	H	H	H	H	H	C	5.1
6	H	H	H	H	H	H	H	I	I	I	I	I	C	C	4.8
7	I	I	I	I	I	H	H	H	H	H	H	C	C	C	4.8
Cluster S3															
1	C	C	H	H	H	H	H	H	H	H	H	H	H	C	33.2
2	C	C	H	H	H	H	H	H	H	H	H	H	C	C	11.3
3	T	T	T	G	G	G	C	H	H	H	H	H	C	C	8.4
4	T	T	T	H	H	H	H	H	H	H	H	H	H	C	6.6
5	T	T	T	G	G	G	C	H	H	H	H	H	C	C	6.6
6	T	T	T	T	H	H	H	H	H	H	H	H	H	C	5.9
7	T	T	T	H	H	H	H	H	H	H	H	H	C	C	5.7

Cluster identification number is given at the first column, peptide sequence and secondary structure assignment at columns 2–15 and the corresponding percentage of occurrence during MD trajectory is displayed at the last column.

^a H stands for α -helix, I stands for π -helix, G stands for 3_{10} -helix, T stands for turn and C stands for coil conformation as computed with the STRIDE program.

Table 5

Hydrogen bond occurrence between individual backbone peptide donors (amide groups) and backbone acceptors (carboxyl groups)

Donor <i>i</i>	Acceptor		
	<i>i</i> – 3	<i>i</i> – 4	<i>i</i> – 5
Lys107	19	–	–
Trp108	8	69	–
Gln109	5	51	46
Glu110	4	32	69
Glu111	4	29	75
Met112	2	27	80
Glu113	4	26	77
Leu114	1	52	71
Tyr115	0	35	77
Arg116	0	25	96
Gln117	0	3	97

Percentage out of the total number of frames that a specific hydrogen bond occurrence is given.

contrary, only 2–4 hydrogen bonds of the pattern $i \leftarrow i + 4$ are in presence. It should be noted that a large number of the hydrogen bonds are bifurcated, a well-known situation for helical conformation in peptides and proteins [35,36]. In agreement with previously analyzed results about the secondary structure, the N-terminal part had a stronger preference for α -helix than the C-terminal. This is evident from the higher percentages of $i, i + 4$ hydrogen bonds found in Phe104–Trp108 and Gln105–Gln109 pairs (Table 5).

The $i \leftarrow i + 5$ hydrogen pattern was not found at all at S2 simulation. In fact 100% of the frames (considering the residues Trp108–Arg116) were found in α -helix.

3.6. Salt bridges

There are numerous possible salt bridges and charge–charge interactions pairs in the peptide sequence that have been reported as essential for apoA-I's functionality [12]. Assuming the helical conformation, three of them might have some role on peptide's conformation stabilization in the context of α -/ π -helix interconversion: (a) Lys106–Glu110, (b) Lys107–Glu111 and (c) Lys106–Glu111. The first two pairs correspond to $i, i + 4$ positions and charge centers might be in close contact in an α -helical conformation. Pair Lys106–Glu111 corresponds to $i, i + 5$ positions, these residues might have strong electrostatic interaction through a π -helical conformation. Times series evaluation of charge–charge distances are shown in Fig. 2.

In both S1 and S2 simulations the Lys106–Glu110 distance remain relatively stable around 1 nm. Trajectory averages values (and variances) where found 1.04 (0.08) and 1.00 (0.11) nm, respectively. The fact that the distance remained relatively constant during the 50 ns trajectory (in the case of the S1) indicates that this did not influenced the α -/ π -helix transition or interconversion. This result is in line with the observation that during S1 trajectory the residues of the N-terminal preferred the α -helical conformation. This can be confirmed from Table 2 where (with the marginal exception of Glu110) these residues populated the α -helical conformation in higher percentages than the π -helix. Thus S1 and S2 trajectories showed similar side chain distance distributions.

Lys107–Glu111 distance was found shorter from the previous one in both trajectories. Trajectory averaged values (Fig. 2) were found 0.63(0.60) and 0.71(0.54) in S1 and S2, respectively.

On the other hand, there is an important feature of the time evolution of the Lys106–Glu111 distance. Its value fluctuated around 1.4 nm during the first 7 ns of the simulation. During the next 2 ns (simultaneously with the α - to π - helical transition of the peptide) the value of the distance dropped down to approximately 0.4 nm. After the 10th ns, this distance oscillates between

0.6 and 1.1 nm, similarly to Lys106–Glu110 and Lys107–Glu111 side chain distances.

Overall, the magnitude of the charge–charge side chain interactions existed in both S1 and S2 simulations was not sufficiently big to support the preference of α - or π -helical conformation due to electrostatic interactions. It is more possible that the shortening of the Lys106–Glu111 side chain distance followed the α - to π -helix transition observed during S1 trajectory rather than it was the cause of this transition.

3.7. Further evidence of the artificial nature of the π -helical conformation

The S1 trajectory (CHARMM22) was extended for a period of 10 ns under the same simulation conditions, but with the CHARMM22/CMAP force field. This frame was found in the TTIIIIIIIICC conformational state. Thus, ten residues in the middle of the peptide sequence were in π -helical conformation. After approximately 150 ps of simulation time, most of the residues were adopted the α -helical conformation and the π -helix was eliminated. The α -helix remained stable for the rest of the simulation time. The transition is also confirmed by the C_α distance of the residues Trp104 and Gln117 (Fig. 2). The value of the distance was raised from 0.15 nm to approximately 0.2 nm, after the first ns of the simulation.

Furthermore, the peptide was build in π -helical conformation (φ, ψ) with backbone dihedral angles set to ($-57^\circ, -70^\circ$), respectively, and solvated with similarly to S1 conditions. Anyway, after 2500 steps of unrestrained energy minimization with the application of the CHARMM22/CMAP force field the peptide lost the initial π -helical conformation and adopted α -helical conformation.

A separate simulation was also run using the AMBER99 force field and the SASA model for implicit representation of the solvent. In this case, conformation of the peptide showed numerous transitions between turn, 3_{10} - and α -helix conformational states, but the π -helical conformation was not observed. Table 3 lists the conformational clusters observed during this simulation (S3). It is evident that α -helix was the dominant conformation of the peptide, with the exception of residues close to N- or C-terminal.

4. Conclusions

Two independent molecular dynamics trajectories of 50 ns have been generated for a helical peptide using the CHARMM22 and CHARMM22/CMAP force fields and the NAMD simulation engine. In the first case significant sampling of π -helical conformation has been recorded. On the other side, application of CHARMM22/CMAP force fields resulted in total elimination of the π -helix observation and the peptide was found in solely α -helical conformation. Despite this helix type interconversion computer simulations of this study provide clear evidence that the fragment 104–117 of apolipoprotein A-I has helical conformation in water. As in other cases found in the literature, the π -helix population during current MD study can be ascribed to CHARM22 force field deficiency to correctly describe the backbone conformation of the peptide, rather than to peptide's preference for π -helix conformation. While π -helices do exist and they have been found experimentally [8] they are quite rare and misconfiguration of computational setup can lead to overestimated π -helix observation in similar computer simulations.

Acknowledgements

Parallel execution of NAMD was performed at the Research Center for Scientific Simulations (RCSS) of the University of Ioannina.

Appendix A. Supplementary material

Supplementary data associated with this article can be found, in the online version, at [doi:10.1016/j.cplett.2008.07.007](https://doi.org/10.1016/j.cplett.2008.07.007).

References

- [1] C.A. Rohl, A.J. Doig, *Protein Sci.* 5 (1996) 1687.
- [2] M.N. Fodje, S. Al-Karadaghi, *Protein Eng.* 15 (2002) 353.
- [3] N. Gibbs, R.B. Sessions, P.B. Williams, C.E. Dempsey, *Biophys. J.* 72 (1997) 2490.
- [4] J.P. Duneau, D. Genest, M. Genest, *J. Biomol. Struct. Dyn.* 13 (1996).
- [5] K.H. Lee, D.R. Benson, K. Kuczera, *Biochemistry* 39 (2000) 13737.
- [6] G.M. Shepherd, D. van der Spoel, H.J. Vogel, *J. Biomol. Struct. Dyn.* 21 (2004) 1.
- [7] N. Sajot, M. Genest, *Eur. J. Biophys.* 28 (2000) 648.
- [8] M. Goetz, C. Carlotti, F. Bontems, E.J. Dufourc, *Biochemistry* 40 (2001) 6534.
- [9] D.M. Morgan, D.G. Lynn, H. Miller-Auer, S.C. Meredith, *Biochemistry* 40 (2001) 14020.
- [10] F.M. Sacks, *Atheroscler. Suppl.* 7 (2006) 23.
- [11] O. Gursky, *Curr. Opin. Lipidol.* 16 (2005) 287.
- [12] A. Chroni, H.Y. Kan, K.E. Kypreos, I.N. Gorshkova, A. Shkodrani, V.I. Zannis, *Biochemistry* 43 (2004) 10442.
- [13] V.K. Mishra, M.N. Palgunachari, *Biochemistry* 35 (1996).
- [14] L.M. Roberts, M.J. Ray, T.W. Shih, E. Hayden, M.M. Reader, C.G. Brouillette, *Biochemistry* 36 (1997).
- [15] A.D. MacKerell et al., *J. Phys. Chem. B* 102 (1998) 3586.
- [16] A.D.J. MacKerell, M. Feig, C.L. Brooks 3rd, *J. Am. Chem. Soc.* 126 (2004) 698.
- [17] H.M. Berman, J. Westbrook, Z. Feng, G. Gilliland, T.N. Bhat, H. Weissing, I.N. Shindyalou, P.E. Bourne, *Nucleic Acids Res.* 28 (2000) 235.
- [18] J.C. Phillips et al., *J. Comput. Chem.* 26 (2005) 1781.
- [19] W. Humphrey, A. Dalke, K. Schulten, *J. Mol. Graph.* 14 (1996) 33.
- [20] W.L. Jorgensen, J. Chandrasekhar, J.D. Madura, R.W. Impey, M.L. Klein, *J. Chem. Phys.* 79 (1983) 926.
- [21] W. Weber, P.H. Hünenberger, J.A. McCammon, *J. Phys. Chem. B* 104 (2000) 3668.
- [22] T. Darden, D. York, L. Pedersen, *J. Chem. Phys.* 98 (1993) 10089.
- [23] A.Y. Toukmaji, J.A. Board Jr., *Comput. Phys. Commun.* 95 (1996) 73.
- [24] W.F. Wilfred, F. van Gunsteren, H.J.C. Berendsen, *Agnew. Chem. Int. Ed. Engl.* 29 (1990) 992.
- [25] E. Barth, K. Kuczera, B. Leimkuhler, R.D. Skeel, *J. Comput. Chem.* 16 (1995) 1192.
- [26] W.G. Hoover, *Phys. Rev. A* 31 (1985) 1695.
- [27] S.E. Feller, Y.H. Zhang, R.W. Pastor, B.R. Brooks, *J. Chem. Phys.* 103 (1995) 4613.
- [28] N.M. Glykos, *J. Comput. Chem.* 27 (2006) 1765.
- [29] D. Frishman, P. Argos, *Proteins* 23 (1995) 566.
- [30] W. Delano, *The PYMOL Molecular Graphics System*, Delano Scientific, San Carlos, CA, 2002.
- [31] J. Wang, P. Cieplak, P.A. Kollman, *J. Comput. Chem.* 21 (2000) 1049.
- [32] J.W. Ponder, *TINKER – Software Tools for Molecular Design*, 2002.
- [33] T. Ooi, M. Oobatake, G. Nemethy, H.A. Scheraga, *Proc. Natl. Acad. Sci. USA* 84 (1987) 3086.
- [34] W.S. Young, C.L. Brooks III, *J. Mol. Biol.* 259 (1996) 560.
- [35] L. Monticelli, D.P. Tieleman, G. Colombo, *J. Phys. Chem. B* 109 (2005) 20064.
- [36] I.Y. Torshin, I.T. Weber, R.W. Harrison, *Protein Eng.* 15 (2002) 359.